

See discussions, stats, and author profiles for this publication at: <https://www.researchgate.net/publication/267814708>

Oxygen Suppresses Light-Driven Anodic Current Generation by a Mixed Phototrophic Culture

ARTICLE in ENVIRONMENTAL SCIENCE AND TECHNOLOGY · NOVEMBER 2014

Impact Factor: 5.33 · DOI: 10.1021/es5024702 · Source: PubMed

CITATIONS

5

READS

33

4 AUTHORS, INCLUDING:



Libertus Darus

University of Queensland

4 PUBLICATIONS 38 CITATIONS

SEE PROFILE



Pablo Ledezma

University of Queensland

20 PUBLICATIONS 119 CITATIONS

SEE PROFILE

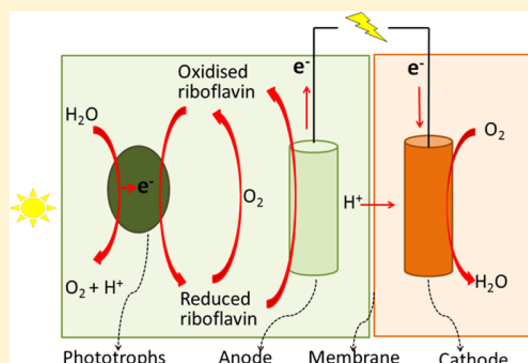
Oxygen Suppresses Light-Driven Anodic Current Generation by a Mixed Phototrophic Culture

Libertus Darus, Pablo Ledezma, Jürg Keller, and Stefano Freguia*

Advanced Water Management Centre, The University of Queensland, St. Lucia, QLD 4072, Australia

Supporting Information

ABSTRACT: This paper describes the detrimental effect of photosynthetically evolved oxygen on anodic current generation in the presence of riboflavin upon illumination of a mixed phototrophic culture enriched from a freshwater pond at +0.6 V vs standard hydrogen electrode. In the presence of riboflavin, the phototrophic biomass in the anodic compartment produced an electrical current in response to light/dark cycles (12 h/12 h) over 12 months of operation, generating a maximum current density of $17.5 \text{ mA}\cdot\text{m}^{-2}$ during the dark phase, whereas a much lower current of approximately $2 \text{ mA}\cdot\text{m}^{-2}$ was generated during illumination. We found that the low current generation under light exposure was caused by high rates of reoxidation of reduced riboflavin by oxygen produced during photosynthesis. Quantification of biomass by fluorescence in situ hybridization images suggested that green algae were predominant in both the anode-based biofilm (55.1%) and the anolyte suspension (87.9%) with the remaining biovolume accounted for by bacteria. Genus-level sequencing analysis revealed that bacteria were dominated by cyanobacterium *Leptolyngbia* ($\sim 35\%$), while the prevailing algae were *Dictyosphaerium*, *Coelastrum*, and *Auxenochlorella*. This study offers a key comprehension of mediator sensitivity to reoxidation by dissolved oxygen for improvement of microbial solar cell performance.



INTRODUCTION

Due to the global issues of fossil fuel depletion and climate change, the development of renewable solar energy-harvesting technologies has gained momentum. Microbial solar cells (MSCs) are an innovative type of bioelectrochemical system (BES), able to turn solar energy into electricity through photosynthetic activity within a fuel cell-type encasing.^{1–3} During photosynthesis in the anodic chamber of a MSC, the light-driven reaction splits water into oxygen, protons and electrons, while CO_2 is concomitantly fixed endogenously into glycogen and new cell material, or protons are reduced into hydrogen by phototrophic microorganisms.⁴ The electrons produced from water splitting^{5,6} and oxidation of intermediate metabolites such as stored glycogen^{7,8} and hydrogen^{9,10} are able to generate an electric current in light and in dark conditions, respectively. The electrons thus generated are used for the reduction of oxygen (or other compounds) in a cathodic chamber.¹¹

MSC anodes containing pure and mixed phototrophic cultures have been successfully tested with and without mediators (added to facilitate electron transfer from the cultures to the anode). Several pure cultures of cyanobacteria have been found to respond electrically in MSCs without the use of mediators, for example, *Synechocystis* spp. (approximately $1.3 \text{ mA}\cdot\text{m}^{-2}$)¹² and *Synechococcus* spp. (approximately $93 \text{ mA}\cdot\text{m}^{-2}$),¹³ but current production has been lower than observed for other BESs. Conversely, the addition of exogenous mediators has resulted in a significant increase in current

output, as is the case for *Anabaena* spp. (approximately $4.5 \text{ A}\cdot\text{m}^{-2}$)⁸ and *Synechococcus* spp. (approximately $400 \text{ mA}\cdot\text{m}^{-2}$)¹⁴ in the presence of 2-hydroxy-1,4-naphthoquinone (HNQ). These investigations usually showed higher current production during the light phase than in the dark. In some cases, however, lower current output was observed during the light phase when mixed phototrophic cultures were employed. He et al.¹⁵ suggested that this effect was due to current generation inhibition caused by photosynthetically evolved oxygen (which can be measured in the form of dissolved oxygen, DO) produced by photosynthesis during the light phase. It is known that DO reduction by biologically derived electrons within the anode chamber of a microbial fuel cell (MFC) prevents extracellular electron transfer to the anode, thus hindering electricity generation,¹⁶ but this effect has not been thoroughly investigated in MSCs.

In this work, we studied the current generation in the presence of riboflavin with a mixed phototrophic bioanode culture as biocatalyst. The use of riboflavin is interesting because it is naturally produced and utilized by bacteria to mediate extracellular electron transfer in biogeochemical metal cycling¹⁷ and in MFC anodes.¹⁸ The self-mediated electron transfer from bacterial cells to MFC anode in the presence of

Received: May 20, 2014

Revised: October 2, 2014

Accepted: November 3, 2014

Published: November 3, 2014



natural consortia was also reported,¹⁹ hence providing an opportunity for a possible synergistic cooperation between chemotrophs and phototrophs in MSCs. This work demonstrates the detrimental effect of oxygen on current generation by a mixed phototrophic culture in the presence of riboflavin during illumination.

■ EXPERIMENTAL SECTION

Microbial Solar Cells Setup. The experiments were conducted in a dark box and used two types of two-chamber photoreactors, flat-plate type and bottle type (described below), illuminated by cool white fluorescent lamps⁶ at the side facing the anode chambers. All experiments were performed in duplicate using two identical reactors. Unless otherwise specified, a 12 h light and 12 h dark phase was maintained by a time-switch controller at $135 \mu\text{mol}\cdot\text{m}^{-2}\cdot\text{s}^{-1}$ light intensity (measured at inner wall of reactors). In order to prevent temperature increase inside the dark box, the box was fitted with two ventilation fans which were operated continuously and hence maintained room temperature conditions ($23\text{--}25^\circ\text{C}$). A modified Cyanophycean medium ($0.05 \text{ g}\cdot\text{L}^{-1} \text{ K}_2\text{HPO}_4$, $0.05 \text{ g}\cdot\text{L}^{-1} \text{ MgSO}_4\cdot 7\text{H}_2\text{O}$, $4.5 \text{ mg}\cdot\text{L}^{-1} \text{ Na}_2\text{EDTA}\cdot 2\text{H}_2\text{O}$, $0.582 \text{ mg}\cdot\text{L}^{-1} \text{ FeCl}_3\cdot 6\text{H}_2\text{O}$, $0.246 \text{ mg}\cdot\text{L}^{-1} \text{ MnCl}_2\cdot 4\text{H}_2\text{O}$, $0.03 \text{ mg}\cdot\text{L}^{-1} \text{ ZnCl}_2$, $0.012 \text{ mg}\cdot\text{L}^{-1} \text{ CoCl}_2\cdot 6\text{H}_2\text{O}$, $0.024 \text{ mg}\cdot\text{L}^{-1} \text{ Na}_2\text{MoO}_4\cdot 2\text{H}_2\text{O}$, and $3.36 \text{ g}\cdot\text{L}^{-1} \text{ NaHCO}_3$ as a buffering agent) at pH 8.0 was fed continuously to the anodic chambers with a syringe pump to maintain a 16-day hydraulic retention time. The cathode chambers were filled solely with phosphate buffer ($6 \text{ g}\cdot\text{L}^{-1} \text{ Na}_2\text{HPO}_4$ and $3 \text{ g}\cdot\text{L}^{-1} \text{ KH}_2\text{PO}_4$) at pH 8.0.

The flat-plate photoreactors were fabricated using four transparent Perspex frames with outer and inner dimensions of $13 \times 28 \times 1 \text{ cm}$ and $5 \times 20 \times 1 \text{ cm}$, respectively. Graphite felt (thickness: 1 mm, Morgan Industrial Carbons, Australia), cation exchange membrane (CEM) (Ultrex CMI-7000, Membrane International) and titanium mesh (mesh size $1 \text{ mm} \times 2 \text{ mm}$, thickness 0.15 mm—Kaian Metal Wire Mesh Co. LTD, China) each with the same surface area of 100 cm^2 were utilized as anode, membrane and cathode materials, respectively (see Supporting Information (SI) Figure S1). The electrolytes in both chambers were continuously circulated using a peristaltic pump with a flow rate $2.5 \text{ L}\cdot\text{h}^{-1}$ via a recirculation system equipped with two 250 mL opaque bottles for anolyte and a 250 mL transparent bottle for catholyte, resulting in total liquid volumes of 600 and 350 mL for anode and cathode chambers, respectively. In the anolyte circulation system, the first bottle (located after the anodic outlet of the photoreactor) functioned as a sample port and housed the online pH and DO sensors. The second bottle, located immediately downstream, was used for gas sparging, release of produced gases and to draw liquid effluent. All circulation bottles were placed in the dark box. To achieve an efficient mixing, the anolyte was continuously stirred at 500 rpm using magnetic bars (diameter 0.5 cm and length 2 cm) in both circulation bottles.

The bottle photoreactors were set up using modified 250 mL borosilicate bottles with the effective volume of anode and cathode chambers solution being 200 cm^3 and 40 cm^3 . Graphite felt (surface area 26 cm^2) was used as anode, directly inserted into the bottle; CEM (4.9 cm^2) was used to separate the anode chamber from a small cathode chamber derived from a glass tube, directly inserted into the bottle; a titanium wire (length 4 cm, diameter 0.5 mm, Advent Research Materials, England) was used as cathode. Platinum wire (length 4 cm, diameter 0.5 mm, Advent Research Materials, U.K.) was used as a cathode in

a specific set of experiments as described in the Results and Discussion section. The bottles were modified with ports to facilitate continuous-flow feeding, to draw liquid effluent, to enable sparging and releasing of gases, and to enable sampling and insertion of pH and DO probes. The use of this bottle type reactor had different aims from the flat plate type reactor and the results are not comparable to each other.

For both reactor types, a Ag/AgCl reference electrode (sat. KCl, $+0.197 \text{ V}$ vs standard hydrogen electrode, SHE) was placed in each anode chamber and Titanium mesh was pressed onto the graphite felt anodes for current collection. The pH of the anolyte was controlled via dosing of 1 M HCl solution to maintain a pH of 8.0 ± 0.2 , using a pump connected to programmable logic controller (PLC) system to provide optimum condition for a microbial consortium performance as biocatalyst,²⁰ to decrease riboflavin photodegradation in the presence of sodium bicarbonate buffer²¹ and to increase solubilization of CO_2 .²²

Analytical Methods. The current density was calculated by dividing the observed anodic current, as recorded by a multichannel potentiostat (CHI1000B, CH Instruments), by the projected anode surface area. The pH and DO were continuously measured by two benchtop pH meters (mini-CHEM-pH, Australia) and a benchtop DO meter (O_2 -4100-e, Mettler Toledo, Germany), and recorded through the PLC system. To determine microbial density of cultures in the anolyte, OD_{660} was measured by spectrophotometer (Cary50 UV-vis, Varian, Australia). The light intensity was measured in $\text{W}\cdot\text{m}^{-2}$ using an IR light sensor (PS-2148, PASPort) and converted to $\mu\text{mol}\cdot\text{m}^{-2}\cdot\text{s}^{-1}$ unit.

16S-rRNA Gene Pyrosequencing, Fluorescence In Situ Hybridization and Biovolume Fraction. In order to identify the stabilized microbial community performing long-term and reproducible electrochemical activities, biomass attached to anodes as biofilm as well as the suspended cultures in the anolyte of one flat plate reactor were collected 12 months after inoculation by scraping the whole anode surface and centrifuging 200 mL of anolyte. Twenty-five mg of either the biofilm or centrifuged suspended culture were used for 16S-rRNA gene pyrosequencing analysis and FISH.

For pyrosequencing, DNA of both samples was extracted using the FastDNA SPIN Kit for Soil (MP Biomedicals, Santa Ana, CA). Extracted DNA was measured for quantity using a NanoDrop ND-1000 spectrophotometer (Nano-Drop Technology, Rockland, DE) and quality using agarose gel (1.0%, w/v electrophoresis). Each extracted DNA was sent to the Australian Centre for Ecogenomics (ACE) at the University of Queensland for 16S-rRNA gene pyrosequencing analysis, using universal primers 926f ($5'$ -AAACTYAAKGAATTGACGG-3') and 1392r ($5'$ -ACGGGCGGTGTGTAC-3')²³ with a 454 GS FLX sequencer (Roche, Switzerland), targeting the 16S rRNA gene regions of the whole community. Sequencing results were analyzed through a local implementation of the ACE Pyrosequencing Pipeline (<https://github.com/Ecogenomics/APP>). Principally, sequences were demultiplexed and quality filtered by the `split_library.py` script in QIIME v1.8.0.²⁴ Sequences shorter than 250bp were removed. Sequences were denoised as well as error-corrected with Acacia.²⁵ Each sequence was aligned by PyNAST²⁶ and assigned to operational taxonomic units (OTUs) using UCLUST²⁷ based on 97% similarity. Taxonomy classifications were then assigned to each OTU by BLAST.²⁸ OTUs identified as chloroplast were filtered out.

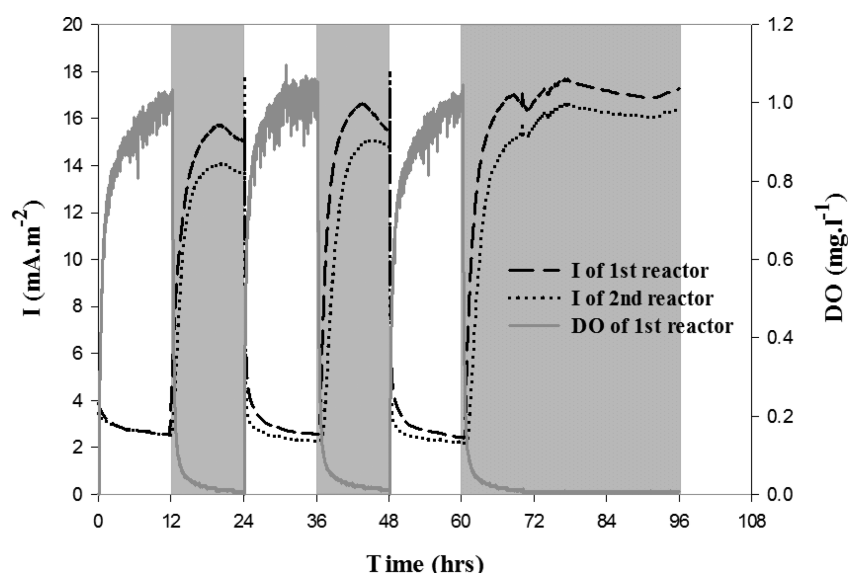


Figure 1. Anodic current profile of two identical flat-plate photoreactors (I of 1st and 2nd reactors, $E = +0.6$ V vs SHE) and DO profile only measured in the 1st reactor, after >12 months exposure to riboflavin; the dark and clear areas symbolize the dark/light phases.

Moreover, the FISH was conducted as described in Amann et al.²³ with hybridization buffer containing 35% of formamide. EUB mix-cy3 probe containing Eub338 (5'-GCTGCCTCCCGTAGGAGT-3'), Eub338II (5'-GCAGC-CACCCGTAGGTGT-3') and Eub338III (5'-GCTGCCACCCGTAGG TGT-3') for most Bacteria^{29,30} and fluorescing stain 4',6-diamidino-2-phenylindole (DAPI) for total microbial cells³¹ were used in this study. Visualization of FISH slides was performed with a Zeiss LSM 510 Meta confocal laser-scanning microscope (CLSM) using two excitation channels (545 nm-red emission and 633 nm-blue emission). Subsequently, 10 randomly chosen images of FISH were quantified by Daime software³² to determine biovolume fraction of bacteria to total microbial cells. Bouchez et al.³³ found that evaluating 10–12 images provided enough total biomass for reliable statistics.

MSC Experimental Procedures. The phototrophic inoculum was collected from a pond (approximately S 27° 29' 59.47 E 153° 0' 58.25) located at the St. Lucia campus of the University of Queensland (Brisbane, Australia) and subsequently pregrown in flasks placed on an orbital shaker at 100 rpm (Thermoline Scientific, Australia) at room temperature under aerobic conditions (without air sparging) in Cyanophycan medium without KNO_3 (i.e., with air as the only nitrogen source) to promote the growth of cyanobacteria. During the pregrowth the cultures were illuminated from the top as previously described ($135 \mu\text{mol} \cdot \text{m}^{-2} \cdot \text{s}^{-1}$ intensity measured at flask walls and with a standard 12/12 h light/dark cycle).

After pregrowth for a month, the green homogeneous cell suspension was centrifuged and washed twice with phosphate buffer (composition detailed above) to be used as inoculum for long-term experiments utilizing 0.5 mM riboflavin in two identical flat-plate photoreactors. The high concentration of riboflavin was used to prevent the concentration becoming limiting. Approximately one year after inoculation in the latter, the cultures were taken from the anolyte, centrifuged, washed twice with phosphate buffer and used as inoculum for subsequent experiments with the two identical bottle photoreactors. In the majority of experiments, the anode potential was poised at +0.6 V vs SHE, the compartment sparged with a

95% N_2 /5% CO_2 gas mix (BOC, Australia) as the sole nitrogen source at a rate $0.5 \text{ L} \cdot \text{min}^{-1}$ and $0.3 \text{ L} \cdot \text{min}^{-1}$ for the flat plate and bottle photoreactors, respectively. Before being supplied to anode chambers, the gas mixture was humidified by flowing it through a bottle containing demineralized water to prevent water loss from the anolyte.

RESULTS AND DISCUSSIONS

Anodic Current Generation in the Presence of Riboflavin. Two identical flat-plate photoreactors were fed for 12 months with medium containing 0.5 mM riboflavin and poised to +0.6 V vs SHE anodic potential. Both reactors exhibited observable green phototrophic cultures both in biofilm and suspended forms. The OD_{660} measured in the anolyte was stable around 0.4–0.5 over this period. Figure 1 represents a current profile over a number of light/dark cycles after 12 months of continuous operation. As shown in the figure, these cultures presented different electrical response to light and dark phase conditions. Within the first 2 min of the light phase, the anodic currents dropped and reached a low point (approximately $2 \text{ mA} \cdot \text{m}^{-2}$) during the rest of the light phase. These output levels are below the previously observed in the presence of mediators, such as a maximum of $1 \text{ A} \cdot \text{m}^{-2}$ generated with a *Synechococcus* sp. PCC7942 MSC³⁴ and $4 \text{ A} \cdot \text{m}^{-2}$ generated with *Synechococcus* sp. UTEX2380³⁵ using 2,5-dibromo methyl isopropyl-1,4-benzo-quinone (DBMB) and 2-hydroxy-1,4-naphthoquinone (HNQ), respectively, as mediators. This may be attributed to poor affinity of our mixed phototrophic culture for riboflavin. In contrast to the light phase, the current output during the dark phase increased gradually to a maximum of $17.5 \text{ mA} \cdot \text{m}^{-2}$ and remained constant even during a 36 h-dark phase (see Figure 1). Although the culture could not develop further electrochemical activity to improve current generation, a sustainable current generation was observed with the same pattern of electric response to light and dark phases for over 12 months.

To confirm that the current generation was of biological origin and the exogenous riboflavin played a key role in the electron-transfer mechanism within the anodic chamber, a short test was carried using two identical bottle photoreactors in

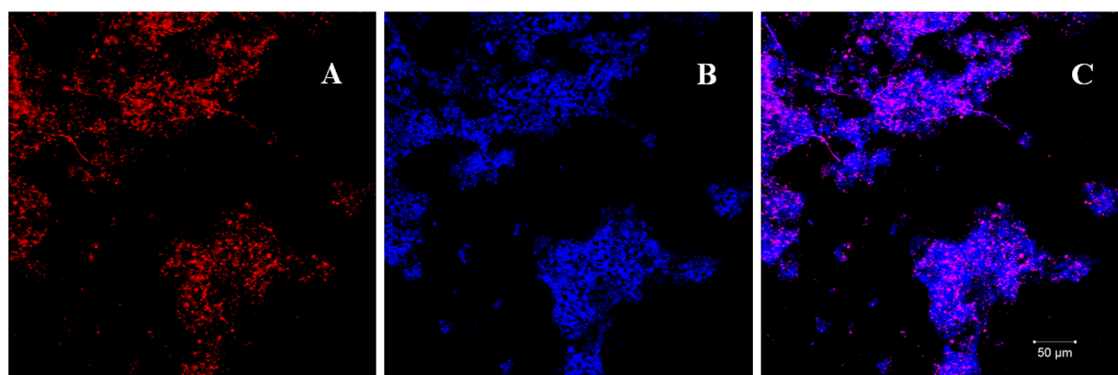


Figure 2. FISH images of the microbial community taken from anode surface. (A, B and C) show the same microscopic field, (A) bacteria in red (EUB mix-probe), (B) nonbacterial cells in blue (after subtraction of total cells stained by DAPI with bacterial cells probed by EUB mix), (C) whole community consisting of bacterial cells in pink as a result of overlapping color of red (EUB mix probe) and blue (DAPI stain) and nonbacterial cells in blue (DAPI), considered to be mainly consisting of microalgae as indicated by sequencing analysis.

continuous mode. When the latter reactors were run abiotically with Cyanophycean medium and poised at +0.6 V vs SHE for 72 h, no electrical response was observed. Subsequently, an anolyte sample from an operating flat-plate photoreactor was collected, centrifuged, washed twice with phosphate buffer. The pellet was then suspended into a 20 mL medium (OD_{660} 8.6) and inoculated into two bottle photoreactors (10 mL each). Following inoculation, an anodic current developed and reached $17 \text{ mA}\cdot\text{m}^{-2}$ during the dark period (though plummeting to $1 \text{ mA}\cdot\text{m}^{-2}$ when illuminated) within the third day of culture addition (see SI Figure S2). The culture used to inoculate these bottle reactors had been exposed to riboflavin for almost a year, so it is possible that some of the cells carried intracellular or membrane bound riboflavin, resulting in the observed current. Within the third day of anolyte replacement with medium containing 0.5 mM riboflavin, the current output increased 10 and 2.2-fold, peaking at 10 and $37 \text{ mA}\cdot\text{m}^{-2}$ during light and dark periods, respectively. There was no electrical response in the absence of a phototrophic culture and the current improved significantly following riboflavin addition, revealing that the culture was responsible for the reduction of oxidized riboflavin and that the anodic oxidation of reduced riboflavin had a primary role in the current production of these photoanodes.

Community Analysis of Biofilm and Suspended Cells.

FISH analyses were conducted to determine the populations of the consortium in both anolyte suspension and anode surface. FISH images of biofilm sample showed the presence of bacteria (see Figure 2A), nonbacterial cells (see Figure 2B) and the whole community (see Figure 2C). Quantification by Daime software showed that the bacteria population occupied 44.9% of the total biovolume fraction in biofilm (100.0 and 10.0% for congruency and standard deviation) and 12.1% of the total microbial biovolume in suspended cells (100.0 and 5.7% for congruency and standard deviation).

Sequence analysis of the consortium in both anode surface and anolyte suspension using universal primers confirmed the presence of bacteria and indicated the presence of green algae. In bacterial community, the prevailing genera were cyanobacterium *Leptolyngbia* accounting for 35.6% in anode surface and 35.0% in anolyte suspension, proteobacteria *Porphyrobacter* (22.9 and 8.9%), *Pseudomonas* (13.5 and 7.8%), *Parvibaculum* (11.9 and 15.2%) and planctomycetes *Rhodopirellula* (16.1 and 33.1%) (see SI Figure S3). At genus level phylogenetically the

green algae were most similar to *Dictyosphaerium*, *Coelastrum*, and *Auxenochlorella*.

Considering the presence of *Leptolyngbia* and green algae we speculate that both phototrophs played a relevant role on the anodic electricity production with riboflavin as mediator. Since only N_2 was supplied as nitrogen source, it is reasonable to hypothesize that the growth of green algae was supported by the cyanobacterium *Leptolyngbia* which has the ability to fix N_2 , providing a nitrogen source for green algae.

He et al.¹⁵ hypothesized that photosynthesis in green algae and cyanobacteria supplied organic compounds as electron donors for heterotrophic bacteria in a MSC. Through oxidation of the organic compounds, heterotrophs (proteobacteria and planctomycetes) might also contribute to electricity production in our systems. Proteobacteria are in fact the main drivers of electricity production in MFCs (e.g., *Geobacter* spp. and *Shewanella* spp.). To the best of our knowledge, of the three proteobacteria found in our systems, only *Pseudomonas*³⁶ has been reported to be electroactive. *Porphyrobacter meromictius* is known as an aerobic anoxygenic phototroph, therefore unable to use water as electron source.³⁷ Although under anaerobic conditions H_2 is known to be produced by photo/chemo-heterotrophic microorganisms,³⁸ no such H_2 -producing microorganisms were present in our community.

The affinity of a culture for a particular mediator in a BES depends on how quickly the oxidized form of the mediator can reach the electron transport chain inside the cells and thereby be reduced.³⁹ In this particular case, the limited affinity can be attributed to the composition of the phototrophic consortium and the impermeability of cell membranes to riboflavin. The complex membrane of the dominant green algae and the lack of a dedicated riboflavin membrane transporter³⁹ might contribute to a low affinity for riboflavin by limiting the migration transport of oxidized riboflavin to diffusive processes across the cell membrane.

Riboflavin Reoxidation by Evolved DO Causes Lower Current Production during the Light Phase. Figure 1 illustrates that the DO increases to a maximum of $1 \text{ mg}\cdot\text{L}^{-1}$ during illumination, coinciding with a sudden current drop, and decreases below detection limits during the dark period. In order to experimentally determine whether the current reduction during light exposure was caused by riboflavin reoxidation by evolved DO, a batch test was conducted and repeated twice in a bottle photoreactor (with Pt-wire cathodes) using the same medium as described in the Experimental

Section with 0.5 mM riboflavin and without phototrophic cultures. The complete reduction of riboflavin was driven at poised-working electrode value of -0.22 V vs SHE in the absence of DO (continuous sparging with N_2). After the reductive current neared zero, the reaction was changed to oxidation by a potential step to $+0.60$ V vs SHE, first in the absence of DO, and then followed by the addition of oxygen (by continuous air sparging). During the reduction and oxidation of riboflavin in the absence of DO, the reductive and oxidative currents decreased logarithmically (see SI Figure S4), which is attributable to the depletion of oxidized and reduced forms of riboflavin, respectively. Oxygen exposure during the oxidation of reduced riboflavin resulted in abrupt decrease in the oxidative current to almost zero, suggesting that the oxidation of the reduced riboflavin was entirely carried out by oxygen. This result reveals that the high sensitivity of reduced riboflavin to DO reoxidation strongly contributed to the poor performance of the pond phototrophic culture when exposed to light.

A similar scenario was observed in MSCs by Tanaka et al.⁷ utilizing HNQ as mediator, suggesting that evolved oxygen could be responsible for the reoxidation of the reduced mediator (HNQ) during the light phase. To confirm that dissolved oxygen was the primary reason for the observed inhibition of current generation in our solar anodes during light exposure, three further tests were conducted: (i) control of DO during light/dark phases; (ii) control of DO during an extended dark phase; and (iii) control of light intensity.

As shown in Figure 3A, 6 h light/dark cycles were performed and simultaneously the DO was gradually decreased from 9 to 1 $mg \cdot L^{-1}$, resulting in a negligible increase of current only reaching 2 $mA \cdot m^{-2}$. The current production only displayed a substantial increase when the DO concentration was taken down to below 1 $mg \cdot L^{-1}$. This is consistent with the results presented in Figure 1, where a DO concentration of 1 $mg \cdot L^{-1}$, due to photosynthetically evolved oxygen, severely limited the current generation during light to around 2 $mA \cdot m^{-2}$.

Due to the continuous oxygen evolution driven by photosynthesis, we were unable to achieve a DO concentration below 1 $mg \cdot L^{-1}$ in the DO control test in our reactor setup during the light period. In the following experiment, a gradual increase of DO (starting from zero) was conducted during an extended dark phase. This experiment, presented in Figure 3B, shows that an increase of the controlled DO results in gradual decrease of the current. There was no current reduction observed due to depletion of the endogenous stored substrate when the reactors were left under an extended dark phase without DO control for 4 days (see SI Figure S5), indicating that the current drop shown in Figure 3B was primarily due to the increase in DO concentration.

Moreover, Figure 3C showed that there is a link between light intensity, photosynthetically evolved DO and generated current in the presence of 0.5 mM riboflavin and a poised anode ($+0.6$ V vs SHE). An increase in light intensity offers more energy for photosynthetic activity and, consequently, more water is split into electrons, protons and oxygen.⁴⁰ As expected, a rapid increase in DO from 0 to 0.3 and then 0.9 $mg \cdot L^{-1}$ was observed when the light intensity was increased from 0 to 55 and then to 135 $\mu mol \cdot m^{-2} \cdot s^{-1}$, respectively (see Figure 3C). As a consequence, the current dropped with the increase of light intensity.

The experimental results demonstrate a univocal link between light, dissolved oxygen and anodic current inhibition

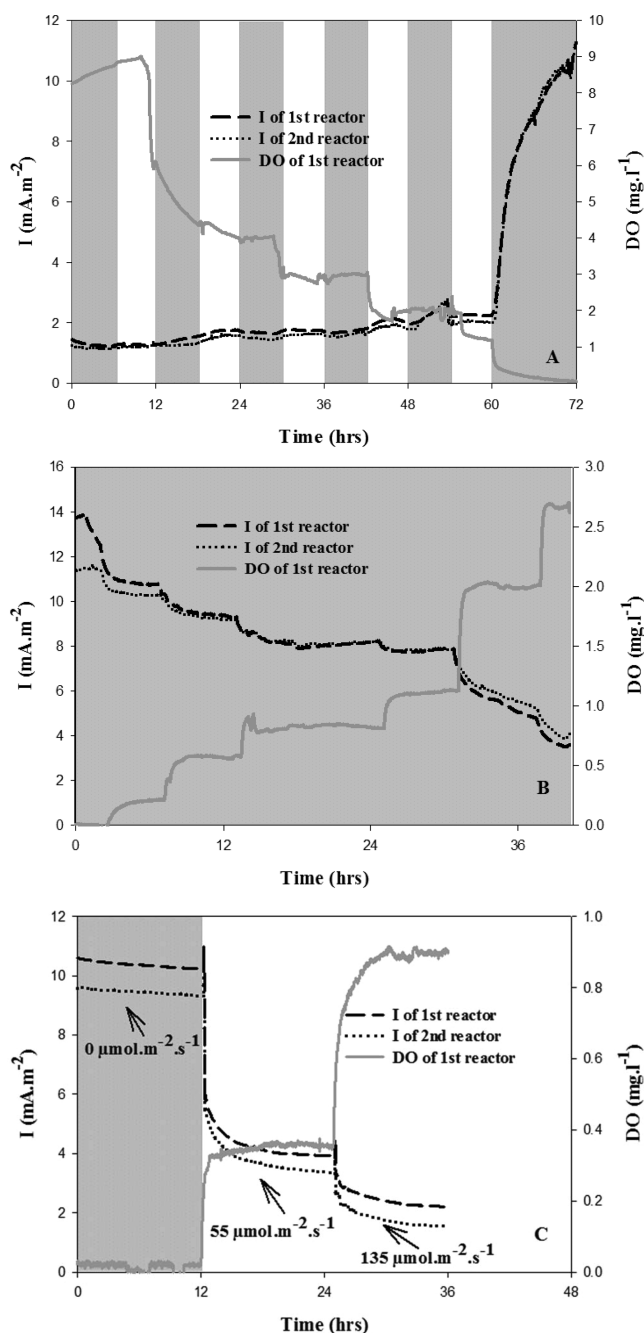


Figure 3. Effect of controlled DO (A, B) and light intensity (C) on anodic current profiles ($E = +0.6$ V vs SHE) of two identical flat plate photoreactors (I of 1st and 2nd reactors) and DO profile (only measured in the 1st reactor) in the presence of 0.5 mM riboflavin. The relatively rough profiles of DO are due to the manual mixing of gases (O_2 and 95% N_2 /5% CO_2 mix).

in mediated photosynthetic bioelectrochemical processes. The high sensitivity of reduced riboflavin to reoxidation by photosynthetically evolved DO detrimentally affects the anodic current during light exposure. Consideration of mediator sensitivity to reoxidation by DO is essential to make MSC a viable technology. Further investigations are warranted to determine the effect of DO on other mediators and on direct electron transfer pathways.

■ ASSOCIATED CONTENT

■ Supporting Information

Figure S1. Pictures of flat-plate and bottle photoreactors. Figure S2. Effect of cultures and riboflavin additions to anodic current profiles in bottle photoreactors. Figure S3. 16S-rRNA gene pyrosequencing analysis of bacteria. Figure S4. Current profiles from redox reactions of riboflavin. Figure S5. Anodic current profile during 4 days dark phase of two identical flat-plate photoreactors. This material is available free of charge via the Internet at <http://pubs.acs.org/>.

■ AUTHOR INFORMATION

Corresponding Author

*Phone: +61 7 3365 4730; fax: +61 7 3365 4726; e-mail: s.freguia@uq.edu.au.

Notes

The authors declare no competing financial interest.

■ ACKNOWLEDGMENTS

This research was funded by the Australian Research Council (ARC DP 120104415). Libertus Darus was supported by the Directorate General of Higher Education (DGHE) of Indonesia and the above ARC project. Stefano Freguia is supported by the fellowship ARC DE130101168. Pablo Ledezma is supported by ARC DP 120104415. We thank Dr. Bernardino Viridis for valuable discussion, Dr. Phil Bond and Dr. Kenn Lu for help with sequencing analyses and FISH, Ampon Chumpia and Markus Fluggen for technical support.

■ REFERENCES

- (1) Freguia, S.; Viridis, B.; Harnisch, F.; Keller, J. Bioelectrochemical systems: Microbial versus enzymatic catalysis. *Electrochim. Acta* **2012**, *82*, 165–174.
- (2) Strik, D. P. B. T. B.; Timmers, R. A.; Helder, M.; Steinbusch, K. J. J.; Hamelers, H. V. M.; Buisman, C. J. N. Microbial solar cells: Applying photosynthetic and electrochemically active organisms. *Trends Biotechnol.* **2011**, *29* (1), 41–49.
- (3) Rosenbaum, M.; He, Z.; Angenent, L. T. Light energy to bioelectricity: Photosynthetic microbial fuel cells. *Curr. Opin. Biotechnol.* **2010**, *21* (3), 259–264.
- (4) Benemann, J. R. Feasibility analysis of photobiological hydrogen production. *Int. J. Hydrogen Energy* **1997**, *22* (10–11), 979–987.
- (5) Zou, Y.; Pisciotto, J.; Billmyre, R. B.; Baskakov, I. V. Photosynthetic microbial fuel cells with positive light response. *Biotechnol. Bioeng.* **2009**, *104* (5), 939–946.
- (6) Pisciotto, J. M.; Zou, Y.; Baskakov, I. V., Light-dependent electrogenic activity of cyanobacteria. *PLoS One* **2010**, *5*, (5).
- (7) Tanaka, K.; Tamamushi, R.; Ogawa, T. Bioelectrochemical fuel cells operated by the cyanobacterium, *Anabaena-variabilis*. *J. Chem. Technol. Biot. B* **1985**, *35* (3), 191–197.
- (8) Tanaka, K.; Kashiwagi, N.; Ogawa, T. Effects of light on the electrical output of bioelectrochemical fuel cells containing *anabaena-variabilis* m-2 - mechanism of the post-illumination burst. *J. Chem. Technol. Biotechnol.* **1988**, *42* (3), 235–240.
- (9) Cho, Y. K.; Donohue, T. J.; Tejedor, I.; Anderson, M. A.; McMahon, K. D.; Noguera, D. R. Development of a solar-powered microbial fuel cell. *J. Appl. Microbiol.* **2008**, *104* (3), 640–650.
- (10) Rosenbaum, M.; Schröder, U.; Scholz, F. In situ electrooxidation of photobiological hydrogen in a photobioelectrochemical fuel cell based on *Rhodobacter sphaeroides*. *Environ. Sci. Technol.* **2005**, *39* (16), 6328–6333.
- (11) Strik, D. P. B. T. B.; Hamelers, H. V. M.; Buisman, C. J. N. Solar energy powered microbial fuel cell with a reversible bioelectrode. *Environ. Sci. Technol.* **2010**, *44* (1), 532–537.
- (12) Madiraju, K. S.; Lyew, D.; Kok, R.; Raghavan, V. Carbon neutral electricity production by *Synechocystis* sp. PCC6803 in a microbial fuel cell. *Bioresour. Technol.* **2012**, *110*, 214–218.
- (13) McCormick, A. J.; Bombelli, P.; Scott, A. M.; Philips, A. J.; Smith, A. G.; Fisher, A. C.; Howe, C. J. Photosynthetic biofilms in pure culture harness solar energy in a mediatorless bio-photovoltaic cell (BPV) system. *Energy Environ. Sci.* **2011**, *4* (11), 4699–4709.
- (14) Yagishita, T.; Horigome, T.; Tanaka, K. Effect of light, CO₂ and inhibitors on the current output of biofuel cells containing the photosynthetic organism *Synechococcus* sp. *J. Chem. Technol. Biotechnol.* **1993**, *56* (4), 393–399.
- (15) He, Z.; Kan, J.; Mansfeld, F.; Angenent, L. T.; Nealsen, K. H. Self-sustained phototrophic microbial fuel cells based on the synergistic cooperation between photosynthetic microorganisms and heterotrophic bacteria. *Environ. Sci. Technol.* **2009**, *43* (5), 1648–1654.
- (16) Harnisch, F.; Schroeder, U. Selectivity versus mobility: Separation of anode and cathode in microbial bioelectrochemical systems. *ChemSusChem* **2009**, *2* (10), 921–926.
- (17) Marsili, E.; Baron, D. B.; Shikhar, I. D.; Coursolle, D.; Gralnick, J. A.; Bond, D. R. *Shewanella* secretes flavins that mediate extracellular electron transfer. *Proc. Natl. Acad. Sci. U. S. A.* **2008**, *105* (10), 3968–3973.
- (18) Li, R.; Tiedje, J. M.; Chiu, C.; Worden, R. M. Soluble electron shuttles can mediate energy taxis toward insoluble electron acceptors. *Environ. Sci. Technol.* **2012**, *46* (5), 2813–2820.
- (19) Rabaey, K.; Boon, N.; Siciliano, S. D.; Verhaege, M.; Verstraete, W. Biofuel cells select for microbial consortia that self-mediate electron transfer. *Appl. Environ. Microbiol.* **2004**, *70* (9), 5373–5382.
- (20) Gil, G. C.; Chang, I. S.; Kim, B. H.; Kim, M.; Jang, J. K.; Park, H. S.; Kim, H. J. Operational parameters affecting the performance of a mediator-less microbial fuel cell. *Biosens. Bioelectron.* **2003**, *18* (4), 327–334.
- (21) Ahmad, I.; Anwar, Z.; Iqbal, K.; Ali, S. A.; Mirza, T.; Khurshid, A.; Khurshid, A.; Arsalan, A. Effect of acetate and carbonate buffers on the photolysis of riboflavin in aqueous solution: A kinetic study. *AAPS PharmSciTech* **2014**, *15* (3), 550–559.
- (22) Sugai-Guérios, M. H.; Mariano, A. B.; Vargas, J. V. C.; de Lima Luz, L. F.; Mitchell, D. A. Mathematical model of the CO₂ solubilisation reaction rates developed for the study of photo-bioreactors. *Can. J. Chem. Eng.* **2014**, *92* (5), 787–795.
- (23) Amann, R. I.; Ludwig, W.; Schleifer, K. H. Phylogenetic identification and in situ detection of individual microbial cells without cultivation. *Microbiol. Rev.* **1995**, *59* (1), 143–169.
- (24) Caporaso, J. G.; Kuczynski, J.; Stombaugh, J.; Bittinger, K.; Bushman, F. D.; Costello, E. K.; Fierer, N.; Pêa, A. G.; Goodrich, J. K.; Gordon, J. I.; Huttley, G. A.; Kelley, S. T.; Knights, D.; Koenig, J. E.; Ley, R. E.; Lozupone, C. A.; McDonald, D.; Muegge, B. D.; Pirrung, M.; Reeder, J.; Sevinsky, J. R.; Turnbaugh, P. J.; Walters, W. A.; Widmann, J.; Yatsunenko, T.; Zaneveld, J.; Knight, R. QIIME allows analysis of high-throughput community sequencing data. *Nat. Meth.* **2010**, *7* (5), 335–336.
- (25) Bragg, L.; Stone, G.; Imelfort, M.; Hugenholtz, P.; Tyson, G. W. Fast, accurate error-correction of amplicon pyrosequences using Acacia. *Nat. Methods* **2012**, *9* (5), 425–426.
- (26) Caporaso, J. G.; Bittinger, K.; Bushman, F. D.; DeSantis, T. Z.; Andersen, G. L.; Knight, R. PyNAST: A flexible tool for aligning sequences to a template alignment. *Bioinformatics (Oxf.)* **2010**, *26*, 266–267.
- (27) Edgar, R. C. Search and clustering orders of magnitude faster than BLAST. *Bioinformatics (Oxf.)* **2010**, *26* (19), 2460–2461.
- (28) Altschul, S. F.; Gish, W.; Miller, W.; Myers, E. W.; Lipman, D. J. Basic local alignment search tool. *J. Mol. Biol.* **1990**, *215* (3), 403–410.
- (29) Amann, R. I.; Binder, B. J.; Olson, R. J.; Chisholm, S. W.; Devereux, R.; Stahl, D. A. Combination of 16S rRNA-targeted oligonucleotide probes with flow cytometry for analyzing mixed microbial populations. *Appl. Environ. Microbiol.* **1990**, *56* (6), 1919–1925.
- (30) Daims, H.; Brühl, A.; Amann, R.; Schleifer, K. H.; Wagner, M. The domain-specific probe EUB338 is insufficient for the detection of

all bacteria: Development and evaluation of a more comprehensive probe set. *Syst. Appl. Microbiol.* **1999**, 22 (3), 434–444.

(31) Porter, K. G.; Feig, Y. S. The use of DAPI for identifying and counting aquatic microflora. *Limnol. Oceanogr.* **1980**, 25 (5), 943–948.

(32) Daims, H.; Wagner, M. Quantification of uncultured microorganisms by fluorescence microscopy and digital image analysis. *Appl. Microbiol. Biotechnol.* **2007**, 75 (2), 237–248.

(33) Bouchez, T.; Patureau, D.; Dabert, P.; Juretschko, S.; Doré, J.; Delgenès, P.; Moletta, R.; Wagner, M. Ecological study of a bioaugmentation failure. *Environ. Microbiol.* **2000**, 2 (2), 179–190.

(34) Tsujimura, S.; Wadano, A.; Kano, K.; Ikeda, T. Photosynthetic bioelectrochemical cell utilizing cyanobacteria and water-generating oxidase. *Enzyme. Microb. Technol.* **2001**, 29 (4–5), 225–231.

(35) Yagishita, T.; Sawayama, S.; Tsukahara, K. I.; Ogi, T. Effects of intensity of incident light and concentrations of *Synechococcus* sp. and 2-hydroxy-1,4-naphthoquinone on the current output of photosynthetic electrochemical cell. *Sol. Energy* **1997**, 61 (5), 347–353.

(36) Rabaey, K.; Boon, N.; Hofte, M.; Verstraete, W. Microbial phenazine production enhances electron transfer in biofuel cells. *Environ. Sci. Technol.* **2005**, 39 (9), 3401–3408.

(37) Rathgeber, C.; Alric, J.; Hughes, E.; Vermeglio, A.; Yurkov, V. The photosynthetic apparatus and photoinduced electron transfer in the aerobic phototrophic bacteria *Roseicyclus mahoneyensis* and *Porphyrobacter meromictius*. *Photosynth. Res.* **2012**, 110 (3), 193–203.

(38) Kapdan, I. K.; Kargi, F. Bio-hydrogen production from waste materials. *Enzyme. Microb. Technol.* **2006**, 38 (5), 569–582.

(39) Yong, Y. C.; Yu, Y. Y.; Yang, Y.; Liu, J.; Wang, J. Y.; Song, H. Enhancement of extracellular electron transfer and bioelectricity output by synthetic porin. *Biotechnol. Bioeng.* **2013**, 110 (2), 408–416.

(40) Lan, J. C. W.; Raman, K.; Huang, C. M.; Chang, C. M. The impact of monochromatic blue and red LED light upon performance of photo microbial fuel cells (PMFCs) using *Chlamydomonas reinhardtii* transformation F5 as biocatalyst. *Biochem. Eng. J.* **2013**, 78, 39–43.